Pergamon

0045-7949(95)00382-7

Computers & Structures Vol. 60, No. 2, pp. 243–260, 1996

0045-7949/96 $15.00 + 0.00

PARAMETRIC STUDIES ON CABLE-STAYED BRIDGES

Pao-Hsii Wang and **Chiung-Guei Yang**
Department of Civil Engineering, Chung-Yuan University, Chung-Li, Taiwan, Republic of China

(*Received* 2 *February* 1995)

Abstract—Parametric studies on cable-stayed bridges are performed in the paper for investigating the individual influence of different sources of nonlinearity in such bridges. The sources of nonlinearity in the cable-stayed bridge mainly include the large deflection, beam–column and cable sag effects. The influence of such kind of effects on the analysis and the structural behavior of cable-stayed bridges has been detailedly examined in the study. A finite element procedure for the nonlinear analysis of cable-stayed bridges is first set up, and then detailed parametric studies for the initial shape analysis and static deflection analysis of such bridges are carried out. The numerical results show that in the initial shape analysis the cable sag effect is most important and the other two effects are insignificant. However, in the static deflection analysis of cable-stayed bridges the large deflection effect plays the key role, the beam–column effect is also significant but minor than the large deflection effect and the cable sag effect becomes the least important one. Copyright © 1996 Elsevier Science Ltd

1. INTRODUCTION

The concept of supporting a bridge deck by inclined tension stays can be traced back to the seventeeth century, but rapid progress in the analysis and construction of cable-stayed bridges has been made over the last 30 years. This progress is mainly due to the developments in the fields of computer technology, high strength steel cables and box-girders with orthotropic steel decks. Since the first modern cable-stayed bridge was built in Sweden in 1955, their popularity has rapidly been increasing all over the world [1–3]. Because of its aesthetic appeal, economic grounds and the ease of erection, the cable-stayed bridge is considered as the most suitable one for medium to long span bridges with spans ranging from 200 m to about 1000 m. In the recent study of Gimsing [4], it is concluded that with new design concepts, e.g. twin girder systems, multi-cable planes and partial earth anchoring of the cable systems, the cable-stayed bridge should be seriously considered as an alternative to the suspension bridge system for even the most extreme spans, e.g. 3200 m. A cable-stayed bridge consists of three principal components, namely girders, towers and inclined cable stays. The girder is supported elastically at points along its length by inclined cable stays so that the girder can span a much longer distance without intermediate piers. The dead load and traffic load on the girders are transmitted to the towers by inclined cable stays. Since the span is large and the cable stays are long and under high pretension force action, the nonlinearities due to cable sag, compression effect in towers and girders and large deflections have to be taken into account. As a result of this the analysis of cable-stayed bridges is becoming very complicated. The purpose of this paper is to present the efficient computational algorithm for finding the initial shape of cable-stayed bridges under the action of the dead load of girders and pretension forces in inclined cables, and for the static deflection analysis under live load action. Parametric studies are performed for investigating the individual influence of the different sources of nonlinearity on the behavior of cable-stayed bridges.

2. NONLINEARITIES OF CABLE-STAYED BRIDGES

The sources of nonlinearity in cable-stayed bridges mainly include the cable sag, beam–column and large deflection effects. They will be briefly explained in the following.

(1) *Cable sag effect*

The inclined cable stay of cable-stayed bridges is generally quite long and it is well known that a cable supported at its end and under the action of its own dead load and axial tensile force will sag into a catenary shape, see Fig. 1. The axial stiffness of a cable will change with changing sag. When a straight cable element for a whole inclined cable stay is used in the analysis, the sag effect has to be taken into account. On the consideration of the sag nonlinearity in the inclined cable stays, it is convenient to use an equivalent straight cable element with an equivalent modulus of elasticity, which can well describe the catenary action of the cable. The concept of a cable equivalent modulus of elasticity was first introduced by Ernst [5].

If the change in tension for a cable during a load increment is not large, the axial stiffness of the cable will not significantly change and the cable equivalent

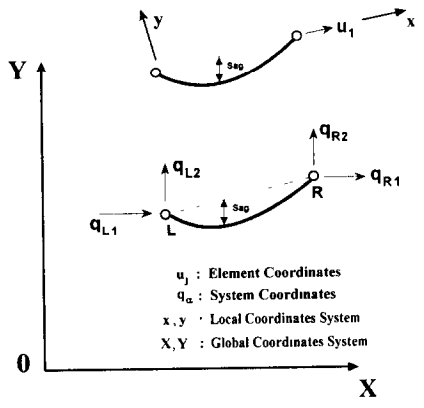

Fig. 1. Cable element with sag.

modulus of elasticity can be considered constant during the load increment and is given by

$$E_{eq} = \frac{E}{1 + \dfrac{(wL)^2 AE}{12T^3}}$$

in which E_{eq} = equivalent cable modulus of elasticity, E = effective cable material modulus of elasticity, A = cross-sectional area, w = cable weight per unit length, L = horizontal projected length of the cable and T = tension force in the cable. The cable equivalent modulus of elasticity combines both the effects of material and geometric deformation. The value of the equivalent modulus is dependent upon the weight and the tension in cable. Hence, the axial stiffness of the equivalent element combining cable sag and cable tension determined by the above equation is the same as the axial stiffness of the actual cable.

When the sag effect exists and the inclined cable stay is represented by a single equivalent straight cable element with one coordinate (relative axial deformation) $u_1 = \Delta l$, see Fig. 1, the stiffness matrix $\mathbf{KE}_{jk}$ of the cable element has the value as follows:

$$\mathbf{KE}_{jk} = [KE] = \begin{cases} \left[\dfrac{E_{eq}A}{l}\right], & \text{for } u_1 > 0 \\ [0], & \text{for } u_1 < 0, \end{cases}$$

where l = cable element length. The cable stiffness vanishes and no element force exists for $u_1 < 0$, i.e. when shortening occurs.

(2) *Beam–column effect*

Since a high pretension force exists in inclined cable stays, the towers and part of the girders are subjected to a large compression action; this means that the beam–column effect has to be taken into consideration for girders and towers of the cable-stayed bridge. In a beam–column, lateral deflection and axial force are interrelated such that its bending stiffness is dependent on the element axial forces, and the presence of bending moments will affect the axial stiffness. The element bending stiffness decreases for a compression axial force and increases for a tension force. The beam–column effect can be evaluated by using the stability functions [6, 7]. The plane beam–column element shown in Fig. 2 is utilized in this study. It has three element coordinates, two for end rotations, u_1, u_2 and one for the relative axial deformation $u_3 = \Delta l$, where Δl is the element axial elongation or shortening. The element forces corresponding to u_j are denoted by S_j in which S_1 and S_2 are the end moments and S_3 is the axial force.

When the beam–column effect has to be taken into consideration, the beam–column element stiffness matrix has the following form [6, 7]

$$\mathbf{KE}_{jk} = [KE] = \frac{EI}{l}\begin{bmatrix} C_s & C_t & 0 \\ C_t & C_s & 0 \\ 0 & 0 & R_t(A/I) \end{bmatrix},$$

where E = modulus of elasticity, A = cross-sectional area, I = moment inertia of the cross-sectional area and l = element length. The stability function C_s, C_t and R_t can be expressed in terms of the element axial force S_3 and the end moments S_1 and S_2 as follows:

(i) For a compressive axial force, $S_3 < 0$

$$C_s = \frac{J[\sin(J) - J\cos(J)]}{2 - 2\cos(J) - J\sin(J)}$$

$$C_t = \frac{J[J - \sin(J)]}{2 - 2\cos(J) - J\sin(J)}$$

$$R_t = \frac{1}{1 - \dfrac{EAR_{cm}}{4S_3^3 l^2}},$$

where

$$J = \sqrt{\frac{|S_3|}{EI}}\, l$$

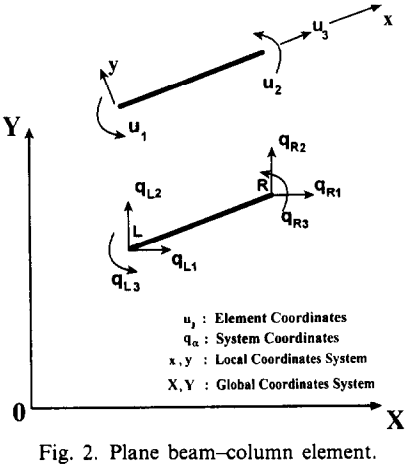

Fig. 2. Plane beam–column element.

$$R_{cm} = J(S_1^2 + S_2^2)[\cot(J) + J\csc^2(J)] - 2(S_1 + S_2)^2 + (S_1 S_2)[1 + J\cot(J)][2J\csc(J)].$$

(ii) For a tensile axial force, $S_3 > 0$

$$C_s = \frac{J[\cosh(J) - J\sinh(J)]}{2 - 2\cosh(J) - J\sinh(J)}$$

$$C_t = \frac{J[\sinh(J) - J]}{2 - 2\cosh(J) + J\sinh(J)}$$

$$R_t = \frac{1}{1 - \dfrac{EAR_{tm}}{4S_3^3 l^2}},$$

where

$$J = \sqrt{\frac{|S_3|}{EI}}\, l$$

$$R_{tm} = J(S_1^2 + S_2^2)[\coth(J) + J\cosh^2(J)] - 2(S_1 + S_2)^2 + (S_1 S_2) \times [1 + J\coth(J)][2J\cosh(J)].$$

When the beam–column effect is not considered, the element stiffness matrix $\mathbf{KE}_{jk}$ of a beam–column element has the linear form as usual as

$$\mathbf{KE}_{jk} = [KE] = \frac{EI}{l}\begin{bmatrix} 4 & 2 & 0 \\ 2 & 4 & 0 \\ 0 & 0 & A/I \end{bmatrix}.$$

(3) *Large displacement effect*

In general, cable-stayed bridges have a larger span and less weight than that of conventional steel and reinforced concrete bridges. Large deflections may easily appear in cable-stayed bridges. Hence, the large displacement effect has to be considered in the analysis and the equilibrium equations must be set up based on the deformed position [8, 9].

In the present study the motion of structural elements during large deflections is described by the exact tranformation coefficients $a_{j\alpha}$ that relate the local element coordinates u_j and the global system coordinates q_α. The nonlinear transformation coefficients of the first-order and the second-order, $a_{j\alpha}$ and $a_{j\alpha,\beta}$, for the straight cable element and the beam–column element can be found in Refs [8, 10]. With the help of the nonlinear transformation coefficients $a_{j\alpha}$ and $a_{j\alpha,\beta}$, the tangent system stiffness matrix will be built up with the standard procedure by assembling the element stiffness matrices (see the next section).

3. NONLINEAR FINITE ELEMENT FORMULATION

Based on the finite element concept, a cable-stayed bridge can be considered as an assembly of a finite number of cable, beam–column (for girder and tower) elements. In this study some assumptions are made as follows. The stress–strain relationship of all material always remains within a linear elastic range during the whole nonlinear computation. The cross-sectional area of the elements remains unchanged during deformation. The cable element is assumed to be perfectly flexible and possesses only tension stiffness; it is incapable of resisting compressive, shear and bending forces. For the beam element, the engineering beam theory is employed and no shear strain is considered. All cables are fixed to the tower and to the girder at their joints of attachment. In the following analysis the nonlinearities induced by beam–column, cable sag and large displacement effects will be taken into account, but all materials behave linearly and elastically.

3.1. *General system equation*

The general system equation for a finite element model of structural systems in nonlinear static analysis can be derived from the virtual work principle and have the following form [8]:

$$\mathbf{K}^J \cdot \mathbf{b}_\alpha^J - \sum_{EL} S_j a_{j\alpha} = 0 \quad \alpha = 1, 2, \ldots, N \text{ DOF}, \quad (1)$$

where

$\mathbf{b}_\alpha^J = \dfrac{\partial \mathbf{W}^J}{\partial q_\alpha}$ = basis vector,

$a_{j\alpha} = \dfrac{\partial u_j}{\partial q_\alpha}$ = transformation coefficients,

$P_\alpha = \mathbf{K}^J \cdot \mathbf{b}_\alpha^J$ = generalized external forces,

$T_\alpha = \sum_{EL} S_j a_{j\alpha}$ = generalized internal forces,

$\mathbf{K}^J$ = external nodal load vectors,

$\mathbf{W}^J$ = displacement vectors corresponding to $\mathbf{K}^J$,

$S_j = \mathbf{KE}_{jk} u_k + S_j^0$ = generalized element forces,

S_j^0 = generalized initial element forces,

u_j = generalized element coordinates,

q_α = generalized system coordinates,

$\mathbf{KE}_{jk}$ = element stiffness matrix,

$\sum_{EL}$ = summation over all elements,

and

N = number of degree of freedom (DOF).

The superscript j denotes the nodal number. The subscripts $\alpha, \beta, \gamma, \ldots$ denote the number of system coordinate and $j, k, l, \ldots$ the number of element coordinate. The index summation convention is used here for the superscripts and subscripts. The letters printed in bold-face type e.g. $\mathbf{K}^j$, $\mathbf{b}'_\alpha$, represent vectors. The dot notation between vectors means scalar product. In the analysis of cable-stayed bridges, the material behaves linearly elastic and the deflection is large, but with small strain. In eqn (1) $\mathbf{b}'_\alpha$, $a_{j\alpha}$, u_j may be nonlinear functions of the system coordinates q_α when large deflections occur and the nodal load vectors $\mathbf{K}^j$ may also become function of q_α, if they are not displacement independent. Equation (1) represents a set of nonlinear algebraic equations and can be solved by the load increment methods or the iteration methods.

3.2. *Linearized system equation*

For the sake of incrementally solving the large deflection problem, the linearized system equation has to be derived. By taking the first order of the Taylor's expansion of the general system eqn (1), the linearized system equation for a small load interval is obtained as follows:

$$\Delta P_\alpha^n + {}_uP_\alpha^n = {}^2K_{\alpha\beta}^n \cdot \Delta q_\beta^n \quad \text{for } P_\alpha^n \leqslant P_\alpha \leqslant P_\alpha^{n+1}, \quad (2)$$

where

$$\Delta P_\alpha^n = P_\alpha^{n+1} - P_\alpha^n = \text{load increments},$$

$$\Delta q_\alpha^n = q_\alpha^{n+1} - q_\alpha^n = \text{displacement increments},$$

$${}_uP_\alpha^n = P_\alpha^n - \sum_{EL} S_j^n a_{j\alpha}^n = \text{unbalanced forces in statics},$$

$${}^2K_{\alpha\beta}^n = \sum_{EL} \mathbf{KE}_{jk}^n a_{j\alpha}^n a_{k\beta}^n + \sum_{EL} S_j^n a_{j\alpha,\beta}^n - {}^n\mathbf{K}^j \cdot {}^n\mathbf{b}'_{\alpha,\beta} - {}^n\mathbf{K}'_\beta \cdot {}^n\mathbf{b}'_\alpha$$

$$= \text{tangent system stiffness matrix},$$

$$a_{j\alpha,\beta} = \frac{\partial a_{j\alpha}}{\partial q_\beta}$$

$$= \text{transformation coefficients of second-order},$$

$$\mathbf{b}'_{\alpha,\beta} = \frac{\partial \mathbf{b}'_\alpha}{\partial q_\beta}.$$

The superscript n denotes the number of load step and the number 2 represents an iteration matrix of the second order. It is well known that a pure increment computation will bring larger numerical errors. An increment-iteration computation procedure is recommended in order to obtain more accurate solutions.

4. ANALYSIS OF CABLE-STAYED BRIDGES

4.1. *Initial shape analysis*

High tension forces exist in cable stays which induce high compressive forces in towers and part of the girders. Since a high pretension force exists in inclined cable stays before live loads are applied, the initial geometry and the prestress of cable-stayed bridges are dependent on each other. They cannot be specified independently as conventional steel or reinforced concrete bridges. Therefore the initial shape, i.e. the geometric configuration and the prestress distribution of cable-stayed bridges, has to be determined prior to analyzing them. The initial shape of a cable-stayed bridge provides the geometric configuration as well as the prestress distribution of the bridge under the action of the dead load of girders and the pretension force in inclined cable stays. The relation for the equilibrium conditions, the specified boundary conditions, and the requirements of architectural design should be satisfied here. For the following shape finding computation, only the dead load of girders is taken into account and the dead load of cables and towers are neglected, but cable sag nonlinearity induced by cable dead load is included. The computation for shape finding starts with a given small tension force in inclined cable stays. Based on a reference configuration (the architectural designed form) having no deflection in girders and zero prestress in any element, the equilibrium position of the cable-stayed bridge under dead load action is first determined iteratively by the Newton–Raphson method. Although this first determined configuration satisfies the equilibrium conditions and the boundary conditions, the requirements of architectural design are generally not fulfilled. Since the bridge span is large and small tension forces exist in inclined cables, quite large deflections and very large bending moments may appear in the girders.

Therefore, a shape iteration has to be carried out in order to reduce the deflection and to smooth the bending moments in the girder. For shape iteration, the axial force of all cable and beam–column elements determined in the previous step will be taken as initial element forces and the equilibrium configuration under the action of dead load and such initial forces will be determined anew. During shape iteration several control points (nodes intersected by the girder and the cable) will be chosen for checking to see if the convergence tolerance is achieved or not. In each shape iteration the ratio of the vertical displacement at control points to the main span length will be checked, i.e.

$$\left| \frac{\text{vertical displacement at control point}}{\text{main span}} \right| \leqslant \epsilon_s$$

The shape iteration will be repeated until the convergence tolerance ϵ_s, say 10^{-4}, is achieved. Numerical experiments show that the iteration

computation converges monotonously. When the convergence tolerance for shape iteration is reached, the computation will be stopped and the initial shape of the cable-stayed bridges is found. A brief summary of the algorithm for shape finding is given in the Section 4.3.1. The details of such a shape finding procedure is referred to Wang *et al.* [10].

4.2. *Static deflection analysis*

Based on the determined initial shape, the nonlinear static deflection analysis of cable-stayed bridges under the live load action can be performed incrementwise or iterationwise. It is well known that the load increment method leads to large numerical errors. The iteration method would be preferred to use for the nonlinear computation and a desired convergence tolerance can be achieved. The Newton–Raphson iteration procedure will be employed in the study.

For nonlinear analysis of large or complex structural systems, a "full" iteration procedure (iteration performed with a singe full load step) will often fail. An increment–iteration procedure is highly recommended, in which the load will be incremented and the iteration will be carried out in each load step. The computaton of nonlinear deflection analysis will be performed with the increment–iteration procedure in this study. The following static deflection analysis of the cable-stayed bridge in different cases will be started from the "exact" initial shape determined by the previously described shape finding procedure, including all the three nonlinearities in the cable-stayed bridge. The algorithm of the static deflection analysis of cable-stayed bridges is summarized in Section 4.3.2.

4.3. *Computation algorithms of the cable-stayed bridge analysis*

The algorithms for shape finding computation and for static deflection analysis of cable-stayed bridges are briefly summarized in the following.

4.3.1. *Initial shape analysis.*

(1) Input the geometric and physical data of the bridge.
(2) Input the dead load of girders and a small initial force in cable stays.
(3) Equilibrium iteration is performed by using the Newton–Raphson Method (see Section 4.3.2)
(4) Shape iteration

(i) Check if the convergence tolerance

$$\left|\frac{\text{vertical displacement at control point}}{\text{main span}}\right| \leqslant \epsilon_s$$

is achieved or not.

(ii) If convergent, then the equilibrium configuration is the desired initial shape else take the determined axial forces as initial element force and repeat steps 3 and 4.

4.3.2. *Static deflection analysis.*

(1) Input the geometric and physical data of the bridge.
(2) Input the initial shape data including initial geometry and initial element forces.
(3) Input the dead and live loads.
(4) Solve the system equation in increment–iteration approach.

(i) Calculate the element stiffness matrices for the cable including sag effect and for the beam–column.

(ii) Calculate the transformation coefficients $a_{j\alpha}, a_{j\alpha,\beta}$.

(iii) Set up the tangent system stiffness matrix, ${}^{2}\mathbf{K}^{n}_{\alpha\beta}$.

(iv) Solve the linearized system equation to find the equilibrium configuration.

(v) Equilibrium iteration (Newton–Raphson approach) is performed as follows:

- After solving the linearized system equations:

$$\Delta P^n_\alpha + {}_u P^n_\alpha = {}^{2}\mathbf{K}^n_{\alpha\beta} \cdot \Delta q^n_\beta,$$

Δq^n_β is found.

- Set $i = 0$,

$${}^{(i)}\Delta q^n_\beta = \Delta q^n_\beta, \; {}^{(i)}q^n_\beta = q^n_\beta,$$

and

$${}^{(i+1)}q^n_\beta = {}^{(i)}\Delta q^n_\beta$$

- If

$$\frac{\|{}^{(i)}\Delta q^n_\beta\|}{\|{}^{(i)}q^n_\beta\|} \leqslant \epsilon \quad \text{(convergence tolerance)}$$

then

$$q^{n+1}_\beta = {}^{(i+1)}q^n_\beta,$$

and begin next load step,
else $i = i + 1$, and solve

$${}^{(i)}_u P^n_\alpha = {}^{(i)}{}^{2}\mathbf{K}^n_{\alpha\beta} \cdot {}^{(i)}\Delta q^n_\beta,$$

with

$${}^{(i+1)}q^n_\beta = {}^{(i)}q^n_\beta + {}^{(i)}\Delta q^n_\beta$$

and repeat convergence tolerance check.

- Determine the element deformations and the element forces.

5. PARAMETRIC STUDIES

The parametric studies made in the paper are focused at investigating the individual influence of the three different sources of nonlinearity, i.e. cable sag,

beam–column and large deflection, on the behavior of cable-stayed bridges. In the following study the solution computed, including all three nonlinearities, will be considered as the "exact" solution and serve as the standard basis for comparisons. The approximate solutions determined by neglecting one of these three nonlinearities will carefully be compared with the "exact" solution in order to investigate the influence of such neglected nonlinearity on the bridge. Four cases of approximate solution are considered in each example studied in Section 6, i.e.

case 1: neglecting cable sag effect (no sag)
case 2: neglecting beam–column effect (no B-C)
case 3: neglecting large deflection effect (no L-D)
case 4: linear case, neglecting all the three nonlinearities (linear).

In cases 1–3 only one kind of nonlinearity is neglected and the other two nonlinearities are taken into account in the analysis. Case 4 is the linear case, in which all the three nonlinearities are neglected and the computation is performed in a pure linear analysis, i.e. the linear elastic element stiffness matrices and linear coordinate transformation coefficients are used in the analysis and no equilibrium iteration is required. For the initial shape analysis all the computations are started from an architectural designed reference configuration of the cable-stayed bridge, i.e. no deflection and no prestress exist in the bridges prior to the analysis. The initial shape is found when the convergence tolerances for both the shape iteration and the equilibrium iteration are achieved. In the linear case (case 4) the equilibrium iteration is not required, but the shape iteration is performed.

After the initial shape is found, the static deflection analysis can be carried out. For the sake of comparisons the "exact" initial shape determined by including all the three nonlinearities is used for the static deflection analysis of all cases. Similarly, the deflection solution including all nonlinearities is considered as the "exact" solution and serves as the basis for comparing the approximate solutions.

6. NUMERICAL EXAMPLES

Three different types of the cable-stayed bridges are taken from the literature. In the following analysis the finite element model of the cable-stayed bridge is idealized by using the cable element with sag shown in Fig. 1 and the beam–column element shown in Fig. 2 and each member located between two nodes is considered as an element. The initial shapes will first be determined by the previous described shape finding procedure. Then, based on the initial shape the deflection analysis of cable-stayed bridges under live loads is performed in increment–iterationwise. Herein a convergence tolerance $\epsilon = 10^{-4}$ is used for both the equilibrium iteration and the shape iteration. During the shape iteration the axial forces of all members of the cable-stayed bridge determined in the previous step will be taken as the initial element force for the next shape iteration. It is different from that made in Ref. [10], where only the cable forces are used as initial element forces for shape iteration. Parametric studies for the initial shape analysis and the static deflection analysis of cable-stayed bridges are performed in each example to investigate the individual influence of the nonlinearities, such as cable sag, beam–column and large displacement effects, on the structural behaviors. The solution determined with including all the three nonlinearities is considered as the "exact" solution. Based on the "exact" solution the approximate solutions will be compared. The approximate solutions are determined by the same computational procedure, but neglecting one of the three major nonlinear effects, e.g. neglecting the cable sag (case 1: no sag), the beam–column (case 2: no B-C) or the large displacement (case 3: no L-D). A linear analysis (case 4: linear) excluding all of the three nonlinearities is also carried out for the sake of comparison in all the examples.

6.1. *Unsymmetrical cable-stayed bridge*

This unsymmetrical cable-stayed bridge is taken from Refs [11, 12]. Its geometrical form and physical properties are shown in Fig. 3. The initial shape of the unsymmetrical cable-stayed bridge is first determined by the previously described algorithm and by taking all the nonlinearities into account. The shape iteration control point is chosen at node 3. Until the initial shape is found, four shape iterations are performed and in each shape iteration five to six cycles in the equilibrium iteration are required. The final geometric configuration and the element forces of the initial shape are listed in Table 1. The pretension forces in cables between nodes 3–5 and 5–10 are 10,010 and 12,043 kips, respectively. The vertical displacement has only 0.018 ft at the control point node 3 and 0.872 ft, 0.40 ft at nodes 2 and 4. The maximum positive and negative bending moment occurs at nodes 2 and 3 and have the value of 44,396 and −71,201 kips-ft, respectively. The initial shape is

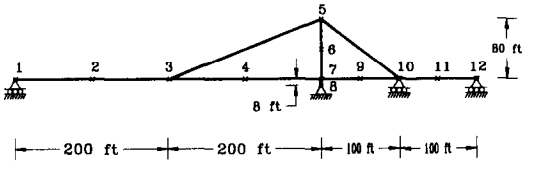

modulus of elasticity E=4,000,000 ksf
girder – I=45.0 ft⁴ ; A=8.0 ft⁴
tower – above girder: I= 20 ft⁴ ; A= 3 ft⁴
below girder: I=200 ft⁴ ; A=10 ft⁴
cable – A=1.1 ft²
dead load – girder W=16.0 kips/ft
cable W= 0.3 kips/ft

Fig. 3. Unsymmetric cable-stayed bridge.

determined again by different approximations (cases 1–4). In this example four shape iterations are required in all cases. The displacements and cable forces determined with different approximations during shape finding are listed in Tables 2–6 and plotted in Fig. 4. From the results it is obviously seen that only the cable sag effect exhibits a significant difference at the initial stages of shape finding and becomes insignificant at the final stage NSI = 4 (NSI = number of shape iterations). The approximate solutions of all cases have good agreement with the exact solution at the final stage. The pretension force in cable elements of all the approximate solutions of the initial shape has almost the same value of the exact solution, and has only an error under 0.1% in this example.

For the static deflection analysis a vertical concentrated load P applied at the node 2 is considered. The load–displacement curves and the load-element force curves are plotted in Fig. 5. From the figures it can be seen that the linear analysis becomes meaningless and the cable sag effect is insignificant in the deflection analysis. The beam–column effect has a significant influence, since the axial force of members has a large value and increases when the deflection increases. The large-deflection effect becomes more important when the deflection becomes large. The convergence difficulty occurs in this example, when the deflection analysis is performed with neglecting the large-deflection effect. The occurrence of the convergence difficulty is denoted by DIV in Fig. 5.

6.2. *Symmetric harp cable-stayed bridge*

This symmetric harp cable-stayed bridge is taken from Refs [11, 13]. Its geometrical and physical properties are given in Fig. 6. Its initial shape is also first determined by the previous described algorithm and by taking all the nonlinearities into account. The shape iteration control points are chosen at nodes 4, 5 and 10. Three cycles in shape iteration are needed until the convergence tolerance is achieved and five to seven cycles of equilibrium iteration in each shape iteration are performed. The convergence in this study is much better than that made in Ref. [10], since the axial forces of all members, instead of only cable forces, of the bridge determined in the previous step are taken as the initial element forces for the next shape iteration computation. Four shape iterations were needed in Ref. [10]. The final geometric configuration and the element forces of the initial shape of the symmetric harp cable-stayed bridge are listed in Table 7. After shape iterations the cable forces converge to 2023, 2361 and 2547 kips in the cable element between the nodes 3–4, 6–5 and 9–10, respectively. The vertical deflection at nodes 4, 5 and 10 (control points) converge to −0.071 ft, −0.11 and 0.01 ft, respectively. The vertical displacement at node 11 (mid-span) is 0.12 ft. The maximum positive and negative bending moments in girder are 14,067 kips-ft at the node 11 and −16,665 kips-ft at the node 10.

The initial shape analysis is repeated for different approximations. In the initial shape analysis of this example three shape iterations have been performed in case 2, case 3 and the case of exact solution. Only two shape iterations are required in cases 1 and 4. The nodal displacements and cable forces of different cases are listed in Tables 8–12 and plotted in Fig. 7. Similar to example 1, neglecting cable sag effect exhibits a significant deviation from the correct value only at the initial stages of shape finding. All the approximate solutions agree well with the exact solution at the final stage (NSI = 3) of shape finding. The cable forces determined in case 2 (no B-C) and case 3 (no L-D) have almost the same value of the exact solution and little difference in cable forces (about 2–13%) exists in case 1 (no sag) and case 4 (linear).

For the deflection analysis, the load–displacement curves and the load-element force curves of each case are plotted in Fig. 8. The results of case 3 (no L-D) have the largest deviation from the exact solution. It means the large deflection effect becomes significant

Table 1. Initial shape of the unsymmetric cable-stayed bridge

Node no.	Reference configuration		Determined configuration		Element no.	Axial force (kips)	Element forces Bending moments (kips-ft)	
	X	Y	X	Y			Left	Right
1	0.00	0.00	−0.02	0.00	3–5	0.100073×10^{5}	—	—
2	100.00	0.00	99.98	0.87	5–10	0.120404×10^{5}	—	—
3	200.00	0.00	199.98	0.02	1–2	0.387060×10^{1}	$-0.727596 \times 10^{-11}$	-0.443965×10^{5}
4	300.00	0.00	299.98	0.40	2–3	0.987206×10^{1}	0.443965×10^{5}	0.712011×10^{5}
5	400.00	−80.00	399.97	−80.00	3–4	-0.928752×10^{4}	-0.712011×10^{5}	-0.284819×10^{5}
6	400.00	−40.00	399.92	−40.00	4–7	-0.928863×10^{4}	0.284819×10^{5}	0.390914×10^{5}
7	400.00	0.00	399.97	0.00	7–9	-0.940245×10^{4}	-0.306044×10^{5}	0.172015×10^{4}
8	400.00	8.00	400.00	8.00	9–10	-0.940220×10^{4}	-0.172015×10^{4}	0.121793×10^{5}
9	450.00	0.00	449.97	−0.03	10–11	0.766528×10^{0}	-0.121793×10^{5}	-0.139103×10^{5}
10	500.00	0.00	499.97	0.00	11–12	0.408693×10^{0}	0.139103×10^{5}	0.139662×10^{-7}
11	550.00	0.00	549.97	0.07	6–5	-0.112387×10^{5}	-0.496437×10^{4}	0.943749×10^{-3}
12	600.00	0.00	599.97	0.00	7–8	-0.112389×10^{5}	-0.883366×10^{4}	0.496347×10^{4}
					8–7	-0.136616×10^{5}	0.685216×10^{-7}	0.346609×10^{3}

Table 2. Vertical displacement at node 2 in shape finding of unsymmetric cable-stayed bridge

	Exact sol.		No sag		No B-C		No L-D		Linear	
NSI	CEI	DISPL. (ft)	CEI	DISPL. (ft)	CEI	DISPL. (ft)	CEI	DISPL. (ft)	CEI	DISPL. (ft)
1	4	3.419	4	2.527	4	3.419	4	3.414	1	2.528
2	5	1.270	5	1.126	4	1.269	5	1.275	1	1.138
3	5	0.926	5	0.903	5	0.924	6	0.930	1	0.913
4	5	0.872	5	0.868	5	0.869	6	0.875	1	0.877

NSI = no. of shape iteration, CEI = cycles of equilibrium iteration

Table 3. Vertical displacement at node 3 in shape finding of unsymmetric cable-stayed bridge

	Exact sol.		No sag		No B-C		No L-D		Linear	
NSI	CEI	DISPL. (ft)	CEI	DISPL. (ft)	CEI	DISPL. (ft)	CEI	DISPL. (ft)	CEI	DISPL (ft)
1	4	3.451	4	2.256	4	3.451	4	3.446	1	2.238
2	5	0.557	5	0.363	4	0.558	5	0.565	1	0.363
3	5	0.091	5	0.060	5	0.092	6	0.097	1	0.059
4	5	0.018	5	0.013	5	0.018	6	0.022	1	0.0095

NSI = no. of shape iteration, CEI = cycles of equilibrium iteration

Table 4. Vertical displacement at node 4 in shape finding of unsymmetric cable-stayed bridge

	Exact sol.		No sag		No B-C		No L-D		Linear	
NSI	CEI	DISPL. (ft)	CEI	DISPL. (ft)	CEI	DISPL. (ft)	CEI	DISPL. (ft)	CEI	DISPL. (ft)
1	4	2.1881	4	1.5767	4	2.1881	4	2.1854	1	1.5329
2	5	0.6846	5	0.5817	4	0.6803	5	0.6885	1	0.5451
3	5	0.4383	5	0.4220	5	0.4354	6	0.4412	1	0.3854
4	5	0.3995	5	0.3970	5	0.3963	6	0.4019	1	0.3595

NSI = no. of shape iteration, CEI = cycles of equilibrium iteration.

Table 5. Cable force of element 3–5 in shape finding of unsymmetric cable-stayed bridge

	Exact sol.		No sag		No B-C		No L-D		Linear	
NSI	CEI	Force (kips)	CEI	Force (kips)	CEI	Force (kips)	CEI	Force (kips)	CEI	Force (kips)
1	4	7700	4	8527	4	7700	4	7674	1	8508
2	5	9654	5	9782	4	9657	5	9645	1	9776
3	5	9959	5	9980	5	9966	6	9955	1	9982
4	5	10007	5	10010	5	10015	6	10004	1	10015

NSI = no. of shape iteration, CEI = cycles of equilibrium iteration.

Table 6. Cable force of element 5–10 in shape finding of unsymmetric cable-stayed bridge

	Exact sol.		No sag		No B-C		No L-D		Linear	
NSI	CEI	Force (kips)	CEI	Force (kips)	CEI	Force (kips)	CEI	Force (kips)	CEI	Force (kips)
1	4	9381	4	10300	4	9381	4	9358	1	10262
2	5	11627	5	11776	4	11629	5	11615	1	11760
3	5	11984	5	12008	5	11992	6	11979	1	12003
4	5	12040	5	12044	5	12050	6	12037	1	12043

NSI = no. of shape iteration, CEI = cycles of equilibrium iteration.

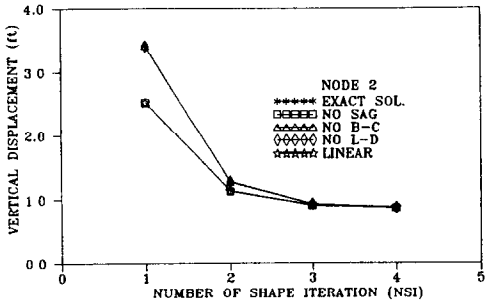

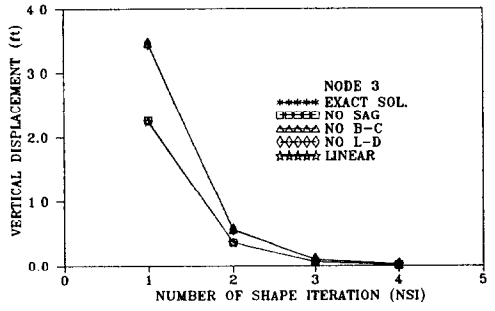

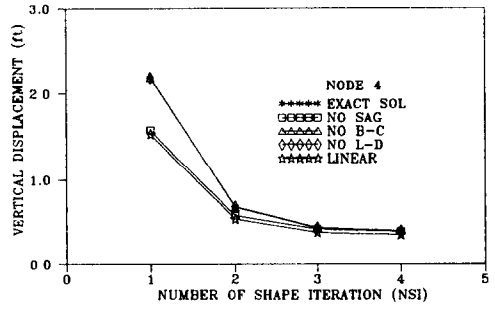

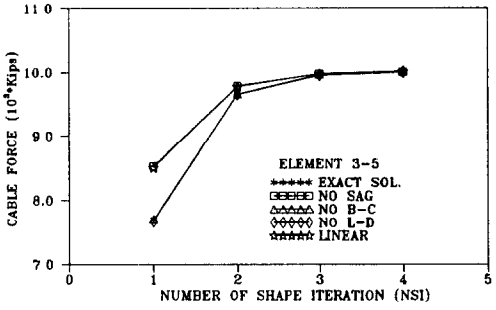

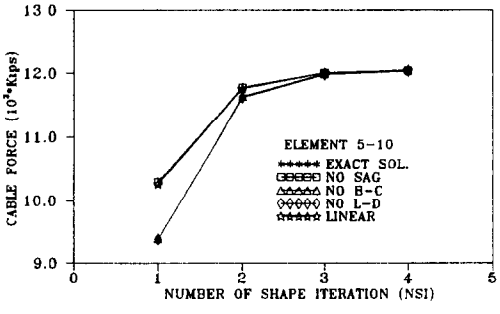

Fig. 4. Shape finding of unsymmetric cable-stayed bridge.

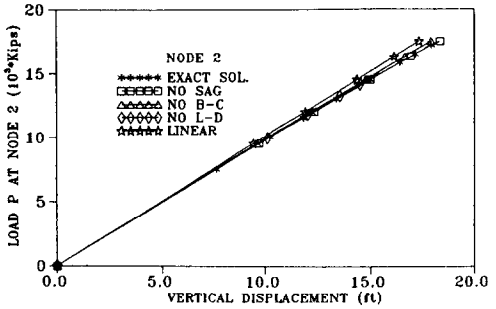

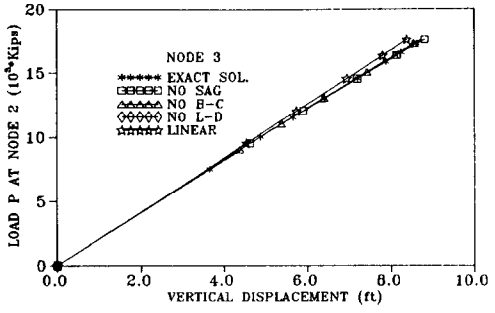

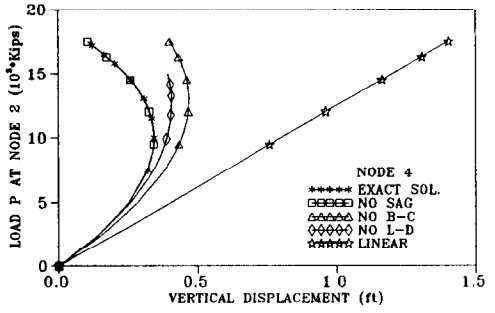

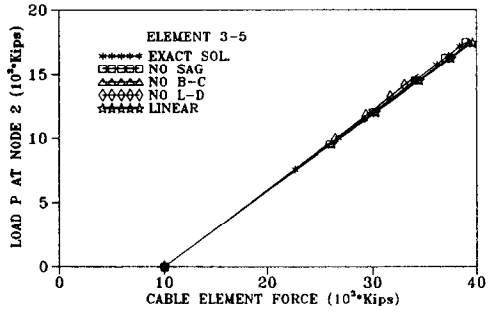

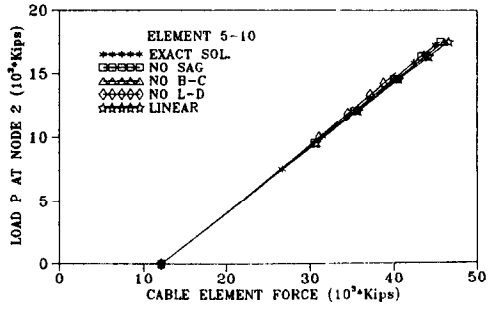

Fig. 5. Static deflection of unsymmetric cable-stayed bridge.

Table 7. Initial shape of the symmetric harp cable-stayed bridge

Node no.	Reference configuration		Determined configuration		Element no.	Axial force (kips)	Element forces Bending moments (kips-ft)	
	X	Y	X	Y			Left	Right
1	450.00	0.00	450.00	0.00	8–9	0.251191×10^4	—	—
2	300.00	0.00	300.00	0.14	7–6	0.240275×10^4	—	—
3	450.00	−66.67	449.96	−66.67	2–3	0.204561×10^4	—	—
4	600.00	0.00	600.00	−0.07	3–4	0.202303×10^4	—	—
5	750.00	0.00	750.00	−0.11	6–5	0.236077×10^4	—	—
6	450.00	−133.34	449.95	−133.34	9–10	0.254709×10^4	—	—
7	150.00	0.00	150.00	0.15	12–13	0.254709×10^4	—	—
8	0.00	0.00	0.00	10.00	17–16	0.236077×10^4	—	—
9	450.00	−200.00	450.00	−200.00	18–19	0.202303×10^4	—	—
10	900.00	0.00	900.00	0.01	19–20	0.204561×10^4	—	—
11	1000.00	0.00	1000.00	0.12	16–15	0.240275×10^4	—	—
12	1100.00	0.00	1100.00	0.01	13–14	0.251191×10^4	—	—
13	1550.00	−200.00	1550.00	−200.00	8–7	-0.229548×10^4	$-0.545697 \times 10^{-11}$	0.880856×10^4
14	2000.00	0.00	2000.00	0.00	7–2	-0.449058×10^4	-0.880856×10^4	0.650520×10^4
15	1850.00	0.00	1850.00	0.15	2–1	-0.635909×10^4	-0.650520×10^4	0.151154×10^5
16	1550.00	−133.34	1550.05	−133.34	1–4	-0.633426×10^4	-0.151704×10^5	0.101110×10^5
17	1250.00	0.00	1250.00	−0.11	4–5	-0.448517×10^4	-0.101110×10^5	0.166645×10^5
18	1400.00	0.00	1400.00	−0.07	5–10	-0.232753×10^4	-0.166645×10^5	0.140674×10^5
19	1550.00	−66.67	1550.05	−66.67	10–11	0.322905×10^0	-0.140674×10^5	-0.159325×10^5
20	1700.00	0.00	1700.00	0.14	11–12	0.322905×10^0	0.159325×10^5	0.140674×10^5
21	1550.00	0.00	1550.00	0.00	12–17	-0.232753×10^4	-0.140674×10^5	0.166645×10^5
					17–18	-0.448517×10^4	-0.166645×10^5	0.101110×10^5
					18–21	-0.633426×10^4	-0.101110×10^5	0.15170×10^5
					21–20	-0.635909×10^4	-0.151154×10^5	0.650520×10^4
					20–15	-0.449058×10^4	-0.650520×10^4	0.880856×10^4
					15–14	-0.229548×10^4	-0.880856×10^4	-0.853834×10^{-8}
					6–9	-0.205466×10^4	-0.224866×10^4	-0.373143×10^{-8}
					3–6	-0.398970×10^4	-0.186111×10^4	0.224866×10^4
					1–3	-0.564287×10^4	0.550307×10^2	0.186111×10^4
					16–13	-0.205466×10^4	0.224866×10^4	-0.234877×10^{-8}
					19–16	-0.398970×10^4	0.186111×10^4	-0.224866×10^4
					21–19	-0.564287×10^4	-0.550285×10^2	-0.186111×10^4

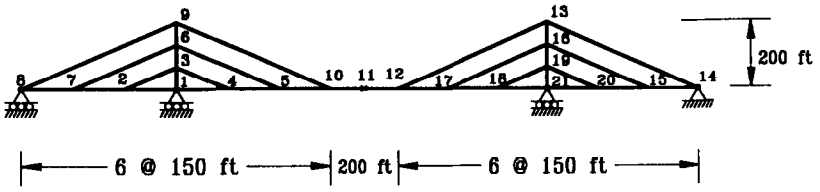

girder, tower E=4,320,000 ksf
cable E=4,320,000 ksf

girder I=131.0 ft^4 : A=3.44 ft^2
tower I=24.4, 40.0, 50.0 ft^4 (from top to buttom)
A=2.18, 2.45, 2.90 ft^2

cable exterior : A=0.452 ft^2
interior : A=0.174 ft^2

dead load girder w=6.0 kips/ft
cable : exterior w=0.221 kips/ft
interior w=0.085 kips/ft

Fig. 6. Symmetric harp cable-stayed bridge.

in static deflection analysis. Only in the cable element between node 2 and 3, do the cable sag and beam–column effects become larger than the large deflection effect, since the cable force decreases when the load increases. There is no great difference in the cable forces of elements 8–9 and 7–6 in all cases.

6.3. *Symmetric radiating cable-stayed bridge*

The symmetric radiating cable-stayed bridge is taken from Ref. [11]. Its geometry is shown in Fig. 9. Its geometric and physical properties have the same values as those of the previous example. The initial shape of the symmetrical radiating cable-stayed bridge is also determined by the previously described algorithm and by taking all the nonlinearities into account. The shape iteration control points are chosen at the nodes 4, 5 and 10. For this example four cycles of shape iteration are needed. In each shape iteration, 4–5 cycles of equilibrium iteration are needed. Similarly, the convergence in this example is better than that made in Ref. [10], since the axial forces of all members are used as the initial element force for the next shape iteration. The final geometric configuration and the element forces of the initial shape of the symmetric radiating cable-stayed bridge are listed in Table 13. The cable forces converge to 1024, 1757 and 2543 kips in the cable elements between the nodes 9–4, 9–5 and 9–10. The vertical deflections at node 4, 5 and 10 converge to -0.0017, -0.0440 and -0.0653 ft, respectively. The vertical displacement at node 11 (mid-span) is 0.172 ft. The maximum positive and negative moment have the value 15,791 and $-16{,}985$ kips-ft at node 11 and 17, respectively.

For the initial shape analysis performed with different approximations four shape iterations are required in case 2 and case 3, but only three shape iterations in case 1 and case 4. The nodal displacements and cable forces are listed in Tables 14–18 and plotted in Fig. 10. Only at the initial stage of shape finding the cable sag effect induces large displacement deviation from the exact solution, but the results of different cases have good agreement at final stage (NSI = 4) of shape finding. Similarly, the cable forces of the approximate solutions have almost the same value of the exact solution and only a little difference (about 3 to 10%) exists in case 4 (linear) exact solution.

For the static deflection analysis the load–displacement curves and the load-element force curves of each case are also plotted in Fig. 11. Similarly the large deflection effect exhibits most significantly. The cable sag and beam–column effects become significant when the cable force discreases, e.g. cable force in element 2–9. There is no great difference in the cable forces of element 8–9 and 7–9 in all cases.

7. CONCLUSIONS

A finite element computation procedure for the initial shape analysis and the static deflection analysis of cable-stayed bridges is presented in the study. The nonlinearities induced by cable sag, beam–column and large displacement effects have been taken into account in the analysis. Parametric studies for investigating the individual influence of such sources of nonlinearity on the analysis of cable-stayed bridges have been carried out in details. From numerical results some conclusions can be made as follows.

I. *For initial shape analysis of cable-stayed bridges*

(1) At the initial stage of shape finding computation the cable-stays have a low tension force, hence, evident displacement deviations from the exact solution appear when the cable sag effect is neglected.

Table 8. Vertical displacement at node 4 in shape finding of harp cable-stayed bridge

	Exact sol.		No sag		No B-C		No L-D		Linear	
NSI	CEI	DISPL. (ft)	CEI	DISPL. (ft)	CEI	DISPL. (ft)	CEI	DISPL. (ft)	CEI	DISPL. (ft)
1	6	1.568	5	0.993	6	1.568	5	1.564	1	0.992
2	5	0.053	6	0.023	5	0.054	5	0.055	1	0.037
3	7	−0.071	—	—	7	−0.070	5	−0.070	1	—

NSI = no. of shape iteration, CEI = cycles of equilibrium iteration.

Table 9. Vertical displacement at node 11 in shape finding of harp cable-stayed bridge

	Exact sol.		No sag		No B-C		No L-D		Linear	
NSI	CEI	DISPL. (ft)	CEI	DISPL. (ft)	CEI	DISPL. (ft)	CEI	DISPL. (ft)	CEI	DISPL. (ft)
1	6	5.335	5	3 001	6	5.335	5	5.322	1	3.006
2	5	0.472	6	0.137	5	0 472	5	0.478	1	0.150
4	7	0.116	—	—	7	0.116	5	0.117	—	—

NSI = no. of shape iteration, CEI = cycles of equilibrium iteration.

Table 10. Cable force of element 8–9 in shape finding of harp cable-stayed bridge

	Exact sol.		No sag		No B-C		No L-D		Linear	
NSI	CEI	Force (kips)	CEI	Force (kips)	CEI	Force (kips)	CEI	Force (kips)	CEI	Force (kips)
1	6	2335	5	2694	6	2335	5	2331	1	2697
2	5	2517	6	2700	5	2517	5	2517	1	2708
4	7	2512	—	—	7	2512	5	2512	—	—

NSI = no. of shape iteration, CEI = cycles of equilibrium iteration.

Table 11. Cable force of element 7–6 in shape finding of harp cable-stayed bridge

	Exact sol.		No sag		No B-C		No L-D		Linear	
NSI	CEI	Force (kips)	CEI	Force (kips)	CEI	Force (kips)	CEI	Force (kips)	CEI	Force (kips)
1	6	2220	5	1891	6	2220	5	2217	1	1886
2	5	2372	6	2100	5	2372	5	2371	1	2093
4	7	2403	—	—	7	2403	5	2402	—	—

NSI = no. of shape iteration, CEI = cycles of equilibrium iteration.

Table 12. Cable force of element 2–3 in shape finding of harp cable-stayed bridge

	Exact sol.		No sag		No B-C		No L-D		Linear	
NSI	CEI	Force (kips)	CEI	Force (kips)	CEI	Force (kips)	CEI	Force (kps)	CEI	Force (kips)
1	6	1821	5	1731	6	1821	5	1819	1	1728
2	5	1987	6	1999	5	1987	5	1987	1	1992
4	7	2046	—	—	7	2045	5	2046	—	—

NSI = no. of shape iteration, CEI = cycles of equilibrium iteration.

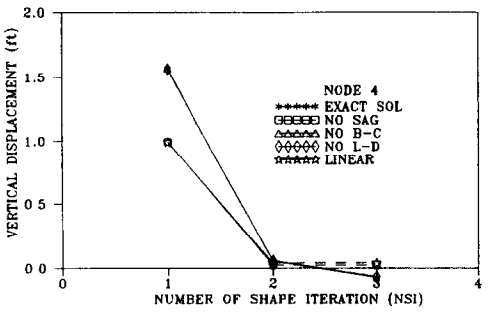

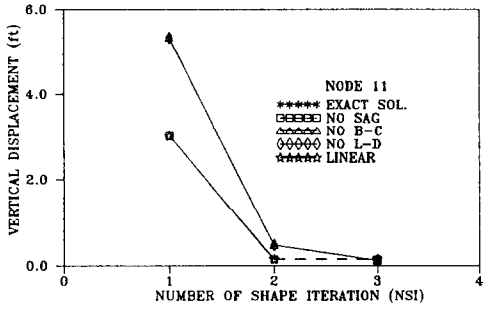

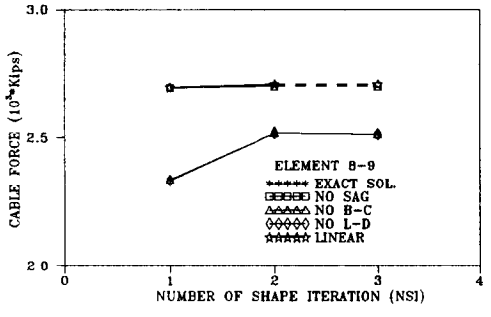

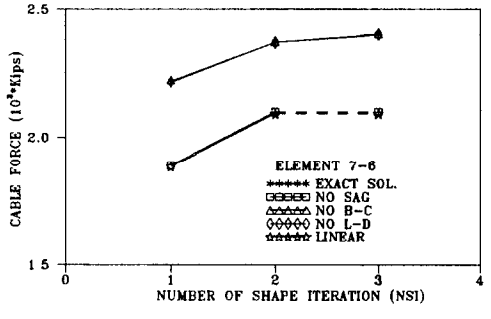

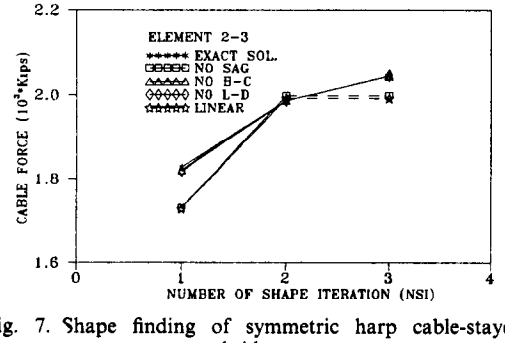

Fig. 7. Shape finding of symmetric harp cable-stayed bridge.

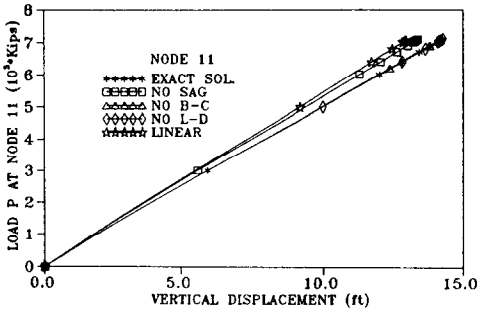

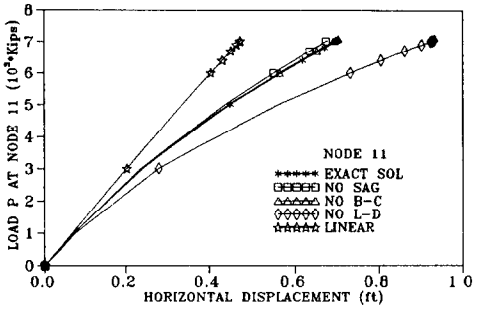

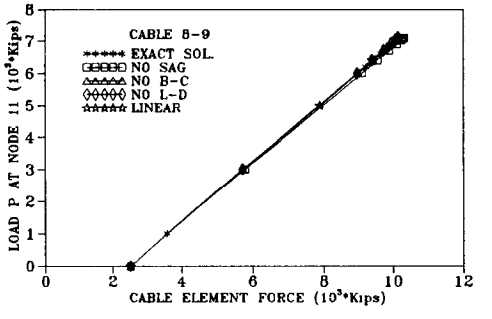

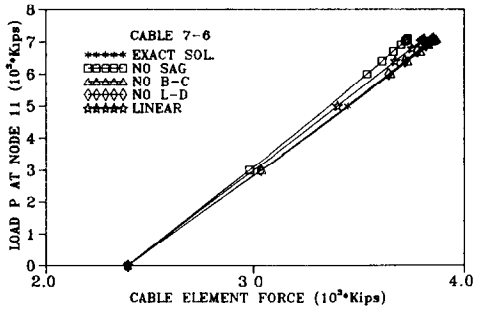

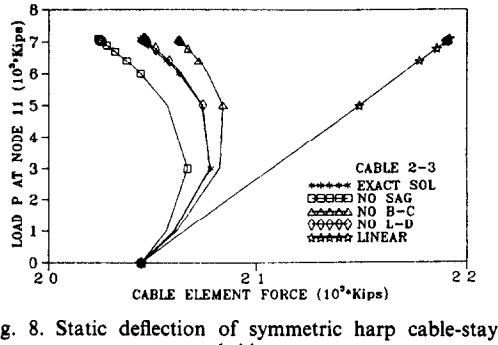

Fig. 8. Static deflection of symmetric harp cable-stayed bridge.

Table 13. Initial shape of the symmetric radiating cable-stayed bridge

Node no.	Reference configuration		Determined configuration		Element no.	Axial force (kips)	Element forces Bending moments (kips-ft)	
	X	Y	X	Y			Left	Right
1	450.00	0.00	450.00	0.00	8–9	0.241554×10^{4}	—	—
2	300.00	0.00	300.00	−0.01	7–9	0.185858×10^{4}	—	—
3	450.00	−66.67	450.01	−66.67	2–9	0.107846×10^{4}	—	—
4	600.00	0.00	600.00	0.00	9–4	0.102386×10^{4}	—	—
5	750.00	0.00	750.00	−0.04	9–5	0.175688×10^{4}	—	—
6	450.00	−133.34	450.01	−133.34	9–10	0.254320×10^{4}	—	—
7	150.00	0.00	150.00	−0.02	12–13	0.254320×10^{4}	—	—
8	0.00	0.00	0.00	0.00	17–13	0.175688×10^{4}	—	—
9	450.00	−200.00	450.01	−200.00	18–13	0.102386×10^{4}	—	—
10	900.00	0.00	900.00	0.07	13–20	0.107846×10^{4}	—	—
11	1000.00	0.00	1000.00	0.17	13–15	0.185858×10^{4}	—	—
12	1100.00	0.00	1100.00	0.07	13–14	0.241555×10^{4}	—	—
13	1550.00	−200.00	1549.99	−200.00	8–7	-0.220734×10^{4}	0.400883×10^{-8}	0.151233×10^{5}
14	2000.00	0.00	2000.00	0.00	7–2	-0.375385×10^{4}	-0.151233×10^{5}	0.105553×10^{5}
15	1850.00	0.00	1850.00	−0.02	2–1	-0.440097×10^{4}	-0.105553×10^{5}	0.115332×10^{5}
16	1550.00	−133.34	1549.99	−133.34	1–4	-0.440007×10^{4}	-0.116718×10^{5}	0.818467×10^{4}
17	1250.00	0.00	1250.00	−0.04	4–5	-0.378575×10^{4}	-0.818467×10^{4}	0.169850×10^{5}
18	1400.00	0.00	1400.00	0.00	5–10	-0.232386×10^{4}	-0.169850×10^{5}	0.142095×10^{5}
19	1550.00	−66.67	1550.00	−66.67	10–11	0.319138×10^{0}	-0.142095×10^{5}	-0.157905×10^{5}
20	1700.00	0.00	1700.00	−0.01	11–12	0.319139×10^{0}	$0\ 157905 \times 10^{5}$	0.142095×10^{5}
21	1550.00	0.00	1550.00	0.00	12–17	-0.232386×10^{4}	-0.142095×10^{5}	0.169850×10^{5}
					17–18	-0.378575×10^{4}	-0.169850×10^{5}	0.818466×10^{4}
					18–21	-0.440007×10^{4}	-0.818466×10^{4}	0.116717×10^{5}
					21–20	-0.440097×10^{4}	-0.115332×10^{5}	0.105553×10^{5}
					20–15	-0.375384×10^{4}	-0.105553×10^{5}	0.151232×10^{5}
					15–14	-0.220734×10^{4}	-0.151232×10^{5}	-0.129148×10^{-9}
					6–9	-0.570134×10^{4}	-0.574174×10^{2}	-0.387899×10^{-6}
					3–6	-0.570134×10^{4}	-0.104728×10^{3}	-0.57417×10^{2}
					1–3	-0.570134×10^{4}	0.138566×10^{3}	-0.104728×10^{3}
					16–13	-0.570134×10^{4}	0.574394×10^{2}	-0.121185×10^{-5}
					19–16	-0.570134×10^{4}	-0.104742×10^{3}	-0.574394×10^{2}
					21–19	-0.570134×10^{4}	-0.138543×10^{3}	-0.104742×10^{3}

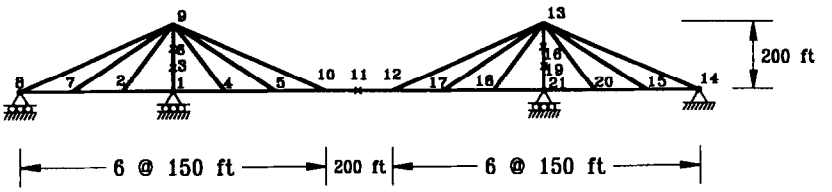

girder, tower E=4,320,000 ksf
cable E=4,320,000 ksf

girder I=131.0 ft^4 : A=3.44 ft^2
tower I=24.4, 40.0, 50.0 ft^4 (from top to buttom)
A=2.18, 2.45, 2.90 ft^2
cable exterior : A=0.452 ft^2
interior : A=0.174 ft^2

dead load girder w=6.0 kips/ft
cable : exterior w=0.221 kips/ft
interior w=0.085 kips/ft

Fig. 9. Symmetric radiating cable-stayed bridge.

Table 14. Vertical displacement at node 4 in shape finding of radiating cable-stayed bridge

	Exact sol.		No sag		No B-C		No L-D		Linear	
NSI	CEI	DISPL. (ft) $\times 10^{-3}$	CEI	DISPL. (ft) $\times 10^{-3}$	CEI	DISPL. (ft) $\times 10^{-3}$	CEI	DISPL. (ft) $\times 10^{-3}$	CEI	DISPL. (ft) $\times 10^{-3}$
1	5	961.18	5	626.63	5	961.18	4	960.13	1	625.21
2	5	−4.12	5	−0.33	5	−3.93	4	−2.81	1	2.74
3	5	−1.86	4	−1.15	5	−1.87	4	−1.85	1	−1.19
4	5	−1.72	—	—	5	−1.82	4	−1.78	—	—

NSI = no. of shape iteration, CEI = cycles of equilibrium iteration.

Table 15. Vertical displacement at node 11 in shape finding of radiating cable-stayed bridge

	Exact sol.		No sag		No B-C		No L-D		Linear	
NSI	CEI	DISPL. (ft)	CEI	DISPL. (ft)	CEI	DISPL. (ft)	CEI	DISPL. (ft)	CEI	DISPL. (ft)
1	4	4.441	5	2.676	5	4.441	4	4.437	1	2.665
2	5	0.656	5	0.302	5	0.655	4	0.660	1	0.312
3	5	0.261	4	0.121	5	0.262	4	0.262	1	0.122
4	5	0.172	—	—	5	0.172	4	0.172	—	—

NSI = no. of shape iteration, CEI = cycles of equilibrium iteration.

Table 16. Cable force of element 8–9 in shape finding of radiating cable-stayed bridge

	Exact sol.		No sag		No B-C		No L-D		Linear	
NSI	CEI	Force (kips)	CEI	Force (kips)	CEI	Force (kips)	CEI	Force (kips)	CEI	Force (kips)
1	5	2103	5	2421	5	2103	4	2100	1	2416
2	5	2337	5	2499	5	2336	4	2336	1	2498
3	5	2392	4	2495	5	2392	4	2392	1	2496
4	5	2416	—	—	5	2415	4	2416	—	—

NSI = no. of shape iteration, CEI = cycles of equilibrium iteration.

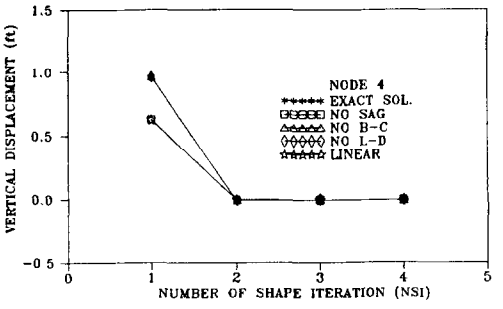

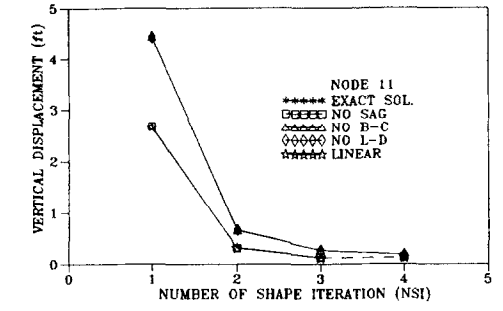

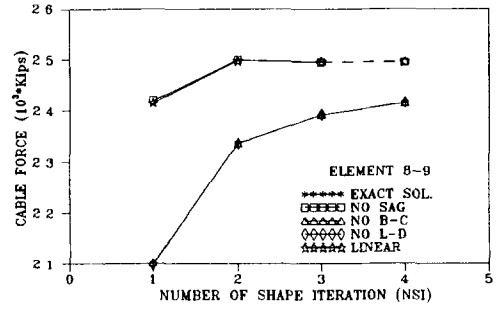

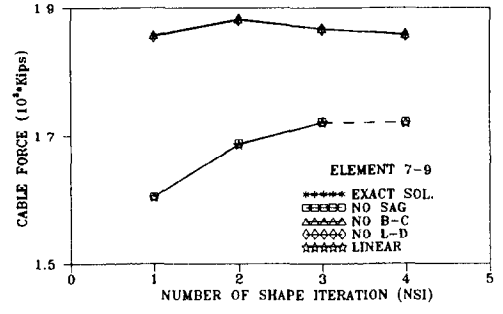

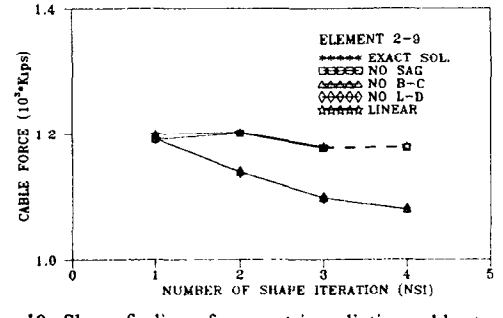

Fig. 10. Shape finding of symmetric radiating cable-stayed bridge.

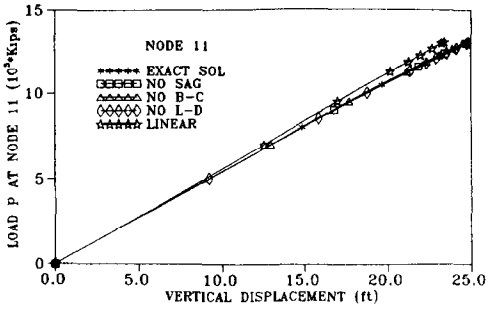

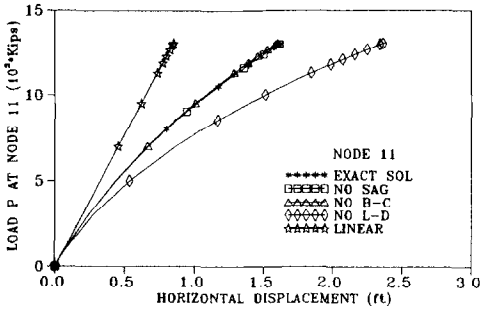

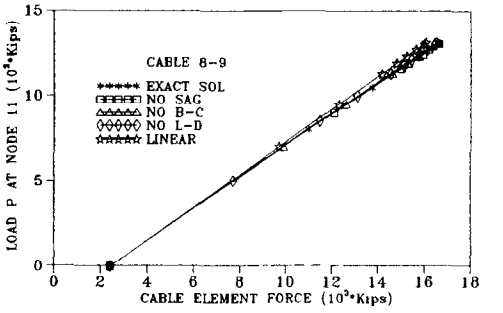

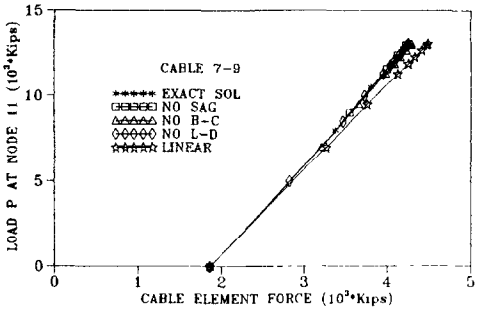

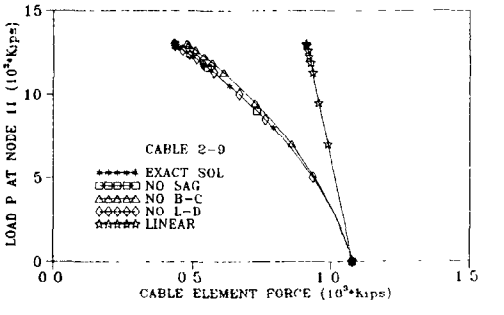

Fig. 11. Static deflection of symmetric radiating cable-stayed bridge.

Table 17. Cable force of element 7–9 in shape finding of radiating cable-stayed bridge

	Exact sol.		No sag		No B-C		No L-D		Linear	
NSI	CEI	Force (kips)	CEI	Force (kips)	CEI	Force (kips)	CEI	Force (kips)	CEI	Force (kips)
1	5	1858	5	1606	5	1858	4	1856	1	1605
2	5	1883	5	1689	5	1883	4	1882	1	1687
3	5	1868	4	1722	5	1868	4	1867	1	1721
4	5	1859	—	—	5	1859	4	1858	—	—

NSI = no. of shape iteration, CEI = cycles of equilibrium iteration.

Table 18. Cable force of element 2–9 in shape finding of radiating cable-stayed bridge

	Exact sol.		No sag		No B-C		No L-D		Linear	
NSI	CEI	Force (kips)	CEI	Force (kips)	CEI	Force (kips)	CEI	Force (kips)	CEI	Force (kips)
1	5	1192	5	1191	5	1192	4	1192	1	1199
2	5	1139	5	1201	5	1140	4	1139	1	1203
3	5	1098	4	1177	5	1098	4	1098	1	1179
4	5	1078	—	—	5	1079	4	1079	—	—

NSI = no. of shape iteration, CEI = cycles of equilibrium iteration.

Since there is a low tension force in the cable-stays, the beam–column effect is also insignificant at the initial stage of shape finding. At the final stage of shape finding all approximate solutions converge to the exact solution and have quite small displacement deviations. That means all the three nonlinearities have less influence on the final geometry of the initial shape.

(2) The beam–column and the large deflection effects have almost no influence on the final cable forces in the initial shape. When the cable sag effect is neglected, about 10% difference in cable forces may appear. Therefore, for cable forces in the initial shape analysis, the cable sag effect is significant, and the beam–column and large deflection effects become insignificant.

(3) A pure linear analysis provides an acceptable result for shape finding computation in which the deviation in deflection is small and the difference in cable forces with respect to the exact solution is about 2–10% only. The linear analysis needs less shape iterations and no equilibrium iteration. A large amount of computation effort can be saved for shape finding. From the point of view of engineering practices, the linear analysis would be highly recommended here for the initial shape analysis of cable-stayed bridges.

(4) During the shape iteration the computation will converge slowly and sometimes becomes difficult to converge when only the axial force of cable-stays determined in the previous step is used as the initial element force for the next shape iteration. A better convergence could be achieved when the axial forces of all members (cable stays, towers and girders) are taken as the initial element force for the computation of the next shape iteration.

II. *For static deflection analysis of cable-stayed bridges*

(1) From the numerical results it is evidently seen that the large deflection effect is the most significant one and has a large influence on the static deflection behavior of cable-stayed bridges. When the large deflection effect is neglected in the deflection analysis an evident deviation from the exact solution will appear and the computation will sometimes become difficult to converge.

(2) The second most significant effect is the beam–column effect. Since large axial forces exist in the members of towers and girders under the dead load and the live load action, the beam–column effect should not be neglected in the static deflection analysis.

(3) The cable-sag effect becomes the least significant one for the static deflection analysis, since large tension forces already exist in the cable-stays under dead load action and their sag becomes quite small. Therefore, only very small change will appear in the deflection of the cable-stayed bridges when the cable-sag effect is neglected, but attention must be paid for that negelecting cable-sag effect will induce error in the determination of the element force of the local cable-stays when the tension force in local cable-stays decreases during the deflection process.

(4) Since large axial forces exist in all the structural members and large deflections occur, a linear analysis for the static deflection analysis of cable-stayed bridges is meaningless and not acceptable.

Acknowledgement—This research was sponsored by a grant under no. NSC 82-0410-E033-08 from the National Science Council, Taiwan, Republic of China.

REFERENCES

1. N. J. Gimsing, *Cable Supported Bridges, Concept and Design*. Wiley, Chichester (1983).
2. F. Leonhardt and W. Zellner, Past, present and future of cable-stayed bridges. In: *Proc. Seminar on Cable-Stayed Bridges, Recent Developments and Their Future*, Yokohama, Japan, 10–11 December, pp. 1–33 (1991).
3. W. J. Podolny and F. Fleming, Historical development of cable-stayed bridges *J. struct. Div. ASCE* **98,** 2079–2095 (1972).
4. N. J. Gimsing, Parametric studies of cable-stayed bridges with extreme spans. In: *Proc. Int. Conf. on Cable-Stayed Bridges*, Bangkok, Thailand (1987).
5. H. J. Ernst, Der E-Modul von Seilen unter Beruecksichtigung des Durchhanges *Der Bauingenieur* **40,** 52–55 (1965).
6. J. F. Fleming, Nonlinear static analysis of cable-stayed bridges. *Comput. Struct.* **10,** 621–635 (1979).
7. A. Ghali and A. M. Neville, *Structural Analysis: A Unified Classical and Matrix Approach* Chapman and Hall, London (1978).
8. K.-H. Schrader, MeSy Einfuehrung in das Konzept und Benutzeranleitung fuer das Programm MESY-MINI, Technisch-Wissenschaftliche Mitteilung Nr. 78-11, Institut Fuer Konstruktiven Inginieurbau, Ruhr-Universitaet Bochum (1978).
9. M. T. Wu, Y. L. Chen and P. H. Wang, Shape finding of cable systems using nonlinear displacement analysis approach. *J. Chin. Inst. Engng* **11,** 583–594 (1988).
10. P. H. Wang, T. C. Tseng and C. G. Yang, Initial shape of cable-stayed bridges. *Comput. Struct* **46,** 1095–1106 (1993).
11. N F Morris, Dynamic analysis of cable-stayed bridges *J. struct. Div. ASCE* **100,** 971–981 (1974).
12. M. C. Tang, Design of cable-stayed girder bridges. *J struct. Div. ASCE* **98,** 1789–1802 (1972)
13. B. E. Lazar, M. S. Troitsky and M. M. Douglass, Load balancing analysis of cable stayed bridges *J. struct. Div ASCE* **98,** 1725–1740 (1972).
14. A. S. Nazmy and A. M. Abdel-Ghaffar, Three-dimensional nonlinear static analysis of cable-stayed bridges. *Comput. Struct.* **34,** 257–271 (1990).
15 M. Ohashi, J. Tajima, M. Yamashita and K Mori, Design of complex cable-stayed bridge. In: *Proc. Int Conf on Cable-Stayed Bridges*, Bangkok, Thailand (1987)
16. A. Rajaraman, K Loganathan and N V. Raman, Nonlinear analysis of cable-stayed bridge. *IABSE Proc.*, P-37/80, pp 205–216 (1980).